Influence of laser pulse duration on extreme ultraviolet and ion emission features from tin plasmas

A. Roy,[1,2,a)] S. S. Harilal,[2] M. P. Polek,[2] S. M. Hassan,[2] A. Endo,[1] and A. Hassanein[2]
[1]*HiLASE Project, Department of Diode-Pumped Lasers, Institute of Physics of the ASCR, Na Slovance 2, 18221 Prague, Czech Republic*
[2]*School of Nuclear Engineering and Center for Materials Under Extreme Environment (CMUXE), Purdue University, West Lafayette, Indiana 47907, USA*

(Received 5 February 2014; accepted 19 March 2014; published online 28 March 2014)

We investigated the role of laser pulse duration and intensity on extreme ultraviolet (EUV) generation and ion emission from a laser produced Sn plasma. For producing plasmas, planar slabs of pure Sn were irradiated with 1064 nm Nd:YAG laser pulses with varying pulse duration (5–20 ns) and intensity. Experimental results performed at CMUXE indicate that the conversion efficiency (CE) of the EUV radiation strongly depend on laser pulse width and intensity, with a maximum CE of ~2.0% measured for the shortest laser pulse width used (5 ns). Faraday Cup ion analysis of Sn plasma showed that the ion flux kinetic profiles are shifted to higher energy side with the reduction in laser pulse duration and narrower ion kinetic profiles are obtained for the longest pulse width used. However, our initial results showed that at a constant laser energy, the ion flux is more or less constant regardless of the excitation laser pulse width. The enhanced EUV emission obtained at shortest laser pulse duration studied is related to efficient laser-plasma reheating supported by presence of higher energy ions at these pulse durations. © *2014 AIP Publishing LLC*.
[http://dx.doi.org/10.1063/1.4870092]

I. INTRODUCTION

Extreme ultraviolet (EUV) radiation from a laser produced tin plasma has been studied extensively in recent years for its potential application as a light source for semiconductor lithography.[1–9] A high-brightness and debris free source emitting at 13.5 nm radiation with 2% bandwidth (in-band) is necessary for this purpose. The selection of EUV source at 13.5 nm is due to the availability of Si-Mo multilayer (ML) mirrors which reflect ~70% of radiation at normal incidence with the bandwidth of 2% centered at 13.5 nm. The need for 13.5 nm wavelength and a regenerative target lead to the use of tin droplet targets.[10] Hot tin plasmas produced by intense laser pulses heated to ~30 eV emit efficient EUV radiation in the in-band region.[11] For EUV lithography source, the power requirement is ~250 W with a brightness $\geq$100 W/(mm^2 sr).[10] The essential requirements of a laser produced plasma (LPP) EUV source are a high conversion efficiency (CE; conversion from laser energy to 13.5 nm with 2% bandwidth) with minimum debris.

The EUV CE from LPP sources strongly depend on laser wavelength, pulse width, spot size, power density, etc. and also on target mass density, target geometry, etc. For the LPP EUV sources, both 1.064 μm Nd:YAG laser and 10.6 μm CO_2 laser are being considered as laser drivers. Nd:YAG laser is a better choice to drive a small EUV source because of its shorter wavelength, which makes it easier to get a small focal spot size and hence better entendue. Spot size is also a very important parameter for LPP EUV light source as it was shown that the spot size affects strongly the plasma expansion and absorption properties.[12]

Previous studies showed that the EUV/x-ray emission from laser-heated clusters are strong function of laser pulse width.[13] The influence of pulse width (fs and ps) on absolute yield measurements of EUV-emission in a wavelength range between 10 nm and 15 nm in combination with cluster target variation were carried out and noted that the ps-laser pulse has resulted in about 30% enhanced and spatially more uniform EUV-emission compared to fs-laser excitation.[14] Ando *et al.*[15] reported that the relative intensity of 13.5 nm emission decreases with increasing angle from plume expansion direction with shortening pulse duration and explained due to change in the opacity of the plasma with laser pulse duration. However, in another experiment[16] it was found that, with laser focal spot sizes from 60 to 270 μm, the in-band CE was almost constant with pulse durations from 0.5 to 15 ns. Tao *et al.*[17] also obtained constant CE from Sn plasmas irradiated with Nd:YAG laser pulse with durations from 0.13 to 30 ns. It was shown that the EUV source size strongly depends on laser intensity instead of laser pulse duration.[17] Ueno *et al.*[18] measured the CE of a CO_2-laser-produced xenon plasma in the EUV spectral region around 13.5 nm at variable laser pulse widths between 200 ps and 25 ns and found that increasing the duration of the laser pulse up to 25 ns results in a gradual increase of EUV CE. Despite large number of theoretical and experimental investigations on the role of laser parameters on EUV CE, the influence of laser pulse duration on EUV CE, spectral features, ion debris are far from complete understanding.

Apart from CE, the cleanness of the EUV LPP sources is extremely important for their use in semiconductor lithography.[19] The EUV LPP source emits debris in the form of

[a)]Author to whom correspondence should be addressed. Electronic addresses: roy@fzu.cz and aroy@barc.gov.in

energetic ions, atoms, and molten droplets.[20] The ablated Sn vapor-deposits on various components, including the surface of the ML mirror, which causes degradation in mirror reflectivity. Several schemes[20] for mitigating the ion and atom debris have been proposed, although they cannot completely mitigate the additional damage from neutrally charged debris.[19] Therefore, it is essential to investigate the energy distribution of Sn ions for various laser pulse widths so that effective debris mitigation schemes can be implemented.

Morris *et al.*[21] reported the angular ion distribution of a tin laser plasma EUV light source over energy/charge state (E/q) ratios ranging from 0.2 to 3 keV. For each individual ion stage detected, more energetic ions showed preferential emission close to the target normal, whereas the less energetic ions exhibited peak emission at larger angles.[21] The effects of laser wavelength (10.6 and 1.064 μm) on the charge state resolved ion energy distributions from Sn LPP expanding into vacuum were investigated and the differences in the ion energy distributions were attributed to the laser wavelength dependence of the laser energy absorption, the resulting plasma density in the corona, and the subsequent recombination after the laser pulse.[22] It was also shown that LPPs exhibit preferential emission close to target normal; the energy of the ions emitted close to the target normal were also higher than that of ions emitted at larger angles.[23] Higashiguchi *et al.*[24] demonstrated suppression of suprathermal ions from a colloidal microjet target plasma containing tin-dioxide (SnO_2) nanoparticles irradiated by double laser pulses. As a result, the peak energy of the singly ionized tin ions was reduced from 9 to 3 keV.[24]

The optimized EUV productions need plasma with appropriate ion populations, which depend strongly on plasma density and temperature. The average charge state Z of an LPP is related to ion kinetic energy (E) and plasma temperature (T_e). Therefore, it is important to study the fast ion distribution for various laser pulse width to gain physical insight of the LPP source.

In this paper, we report the effect of laser pulse width on EUV emission from planar Sn target. Experiments are conducted for four different laser pulse widths with varying laser energy at a laser focal spot size of 80 μm. We analyzed the EUV spectral emission features, CE, with respect to laser intensity and pulse width and correlated to the ion flux and kinetic features from the plasma.

II. EXPERIMENTAL SETUP

A schematic of the experimental setup is shown in Fig. 1. Experiments were carried out using a Q-switched Nd:YAG laser emitting at 1.064 μm in wavelength. Pulse duration was changed from 5 to 20 ns (FWHM) by introducing a delay in the Q-switch. The laser beam energy was attenuated using a combination of a half-wave plate and a polarizing cube. Planar slab of pure Sn was mounted to a servo-motor controlled XYZ translation stage inside a stainless steel high-vacuum chamber. The chamber is evacuated using a turbomolecular pump to a pressure lower than 10^{-5} Torr. A 40 mm plano-convex focusing lens was mounted on micrometer actuator controlled x-translation stage, which allowed tunability of the laser spot size. Laser

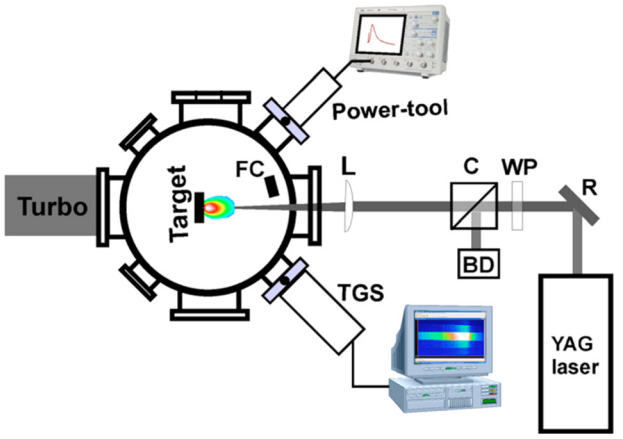

FIG. 1. Schematic of the experimental setup at CMUXE. Optical components include a polarizing cube (C), a half-wave plate (WP), lens (L), reflector (R), and beam dumps (BD). Diagnostic components include a FC; and TGS and EUV power tool. Reprinted with permission from J. Appl. Phys. **108**, 063306 (2010). Copyright 2010 AIP Publishing LLC.[19]

focal spot employed in the experiment was 80 μm. The target was translated between shots to refresh the target surface, and to mitigate the effects of target cratering.

The CE of the incident pulse energy to 13.5 nm radiation was measured with EUV power tool, consisting of two Zr filters and a Mo/Si ML mirror to reflect the incoming plasma light into an absolutely calibrated photodiode. The photodiode signal is then displayed and recorded on an oscilloscope. The planar target geometry emits EUV radiation through a solid angle of 2π steradians. The emission spectrum of Sn plasma was recorded using a transmission grating spectrometer (TGS). The TGS utilizes a silicon nitride diffraction grating with a 10 000 lines/mm resolution. The spectra were then recorded with a EUV sensitive charge coupled device (CCD) camera (Princeton Instruments PIXIS) in a time-integrated manner. The spectral features and CE of EUV emission were monitored at 45° and 90° with respect to target normal. In order to measure the EUV emission from 90° with respect to the target normal the experimental setup has been modified by keeping the positions of TGS and EUV power tool, the target has been rotated such a way that angle of incidence (AOI) is 66° with respect to the target normal. The plasma plume in this case moves in the vertical direction and the TGS and EUV power tool remain in the plane parallel to the target plane.

The fluence and kinetic energy (KE) of the plasma ions were measured with a Faraday cup (FC) mounted inside the vacuum chamber at a distance 15 cm from the target point, at 10° angle from the plane of the beam. The FC was biased with a dc power supply to the optimized potential difference of −31 V. The ion current was measured by acquiring the voltage signal across a load resistor by 1 GHz digital phosphor oscilloscope.

III. RESULTS AND DISCUSSION

A. EUV emission

We evaluated the EUV CE and unresolved transition array (UTA) from laser produced Sn plasma at various pulse durations and laser energies. The dependence of in-band CE

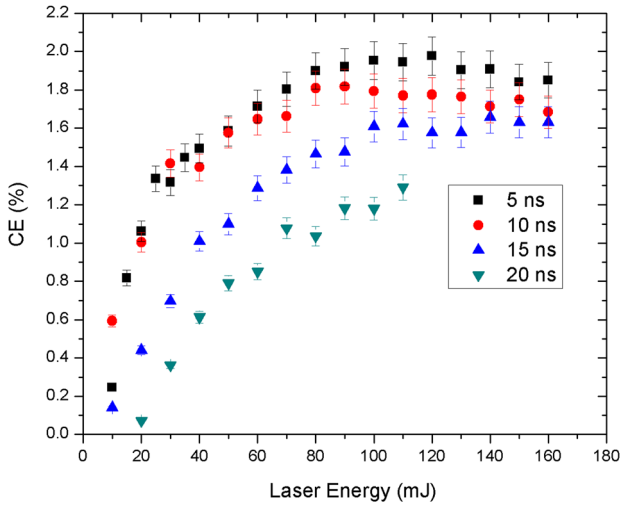

FIG. 2. The dependence of CE on laser energy for various laser pulse widths. For the CE measurement, the power tool was positioned at 45° with respect to target normal and integrated over 2π assuming EUV emission is isotropic.

for four different laser pulse widths (5, 10, 15, and 20 ns) is studied for various laser energies are given in Fig. 2. One can see from Fig. 2 that CE is highly dependent on the laser pulse width as well as laser energy. The spot size at the target surface was fixed at 80 μm regardless of the changes in laser pulse width used and hence the range of laser irradiance used was in the range from 2×10^{10} to 1×10^{12} W/cm^2.

It can be seen from Fig. 2 that the CE increases with laser energy for all laser pulse widths studied; however, maximum CE is obtained for the shortest pulse width used (5 ns FWHM). The maximum CE measured for 5 ns pulse width was ~2%. The obtained peak CE reduces with increase in laser pulse width. With increasing laser energy, the EUV emission enhancement is rapid for shorter laser pulse excitation compared to longer pulse excitations. In LPP, the optimum pulse duration is determined not only by the optical depth but also by a fraction of laser energy absorbed in the EUV emission-dominant region (EDR). In shorter pulse produced plasma, incident laser energy is not directly absorbed in the EDR, but in the denser region because of its steep density gradient. Laser energy absorbed in a dense region is not efficiently converted into output of 13.5 nm light due to its high opacity. For long pulse excitation, multidimensional plasma expansion reduces plasma temperature in the longer pulse laser irradiation cases.[15]

EUV spectra for four different laser pulse widths were recorded with laser pulses of increasing intensity, with a constant spot size of 80 μm, and are given in Fig. 3. EUV spectra shown in Fig. 3(a) for 5 ns laser pulse width have a dip structure around 13.5 nm at higher intensity levels. This dip structure is not very prominent for other laser pulse widths studied. The dip in the UTA was previously reported and attributed to re-absorption of 13.5 nm light by the surrounding plasma.[15] The spectra also show that the dips become shallower as the pulse duration becomes shorter. Fig. 4 displays the EUV

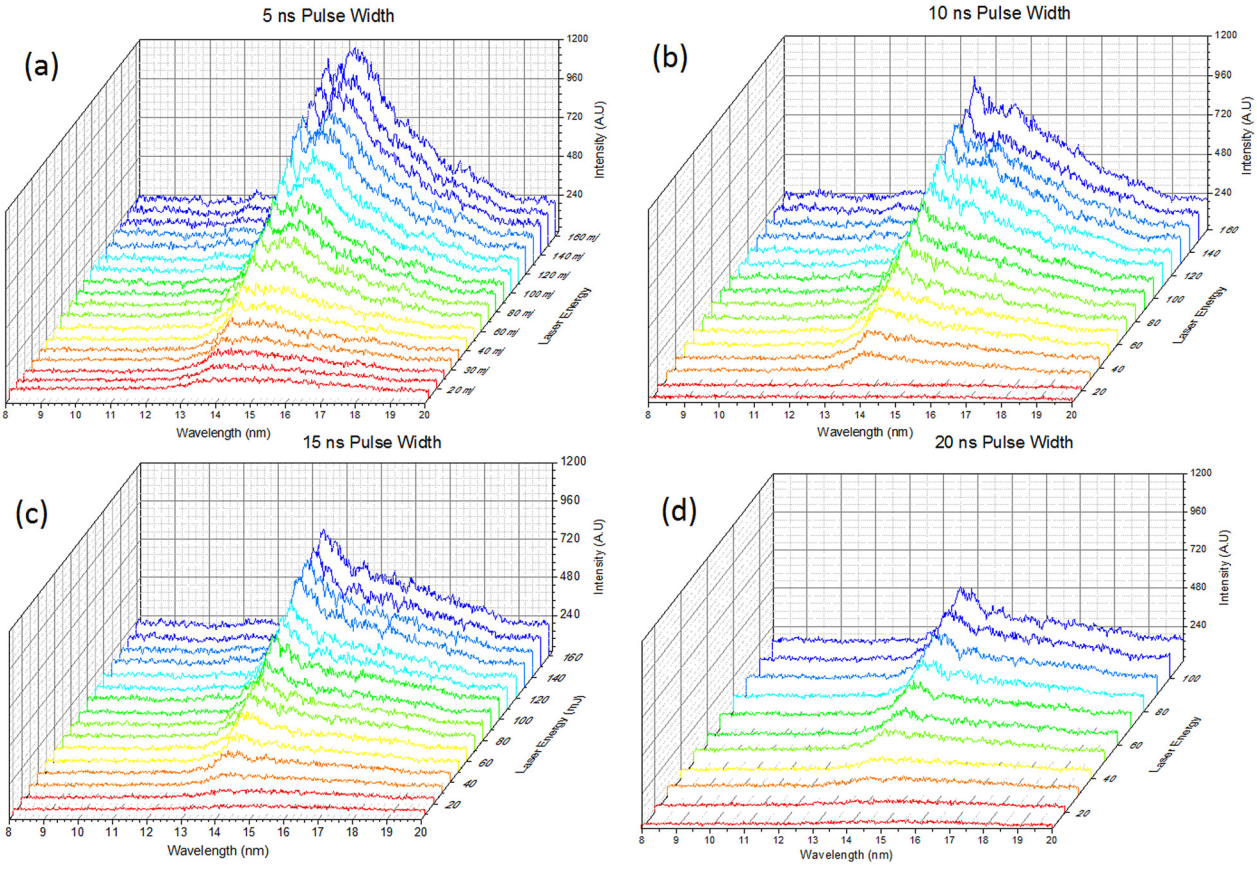

FIG. 3. EUV spectra for four different laser pulse widths recorded with laser pulses of increasing intensity (a) for 5 ns, (b) for 10 ns, (c) for 15 ns, and (d) for 20 ns laser pulse width. For UTA recording, the TGS was positioned at 45° with respect to target normal.

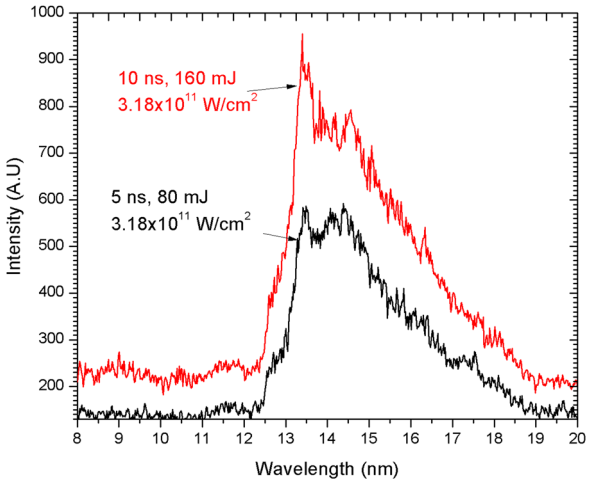

FIG. 4. EUV spectral emission features for various laser pulse widths at same intensity. A transmission grating spectrograph with a resolution of $100(\lambda/\Delta\lambda)$ is used for recording the spectra.

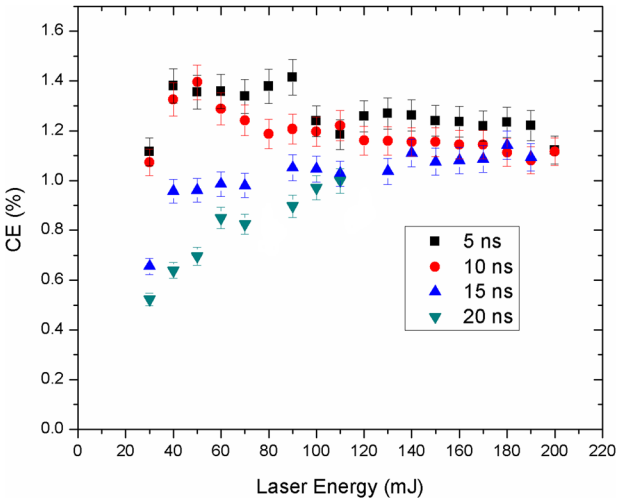

FIG. 5. The dependence of CE on laser energy for various laser pulse widths recorded at 90° with respect to target normal.

spectra for same laser intensity but with different laser pulse widths. One can see form Fig. 4 that the spectral intensity for 5 ns pulse width is 1.6 times lower than that of 10 ns pulse width. However, the spectral dip is much shallower for 5 ns pulse width as compared to 10 ns pulse width. It highlights that the plasma self-absorption is higher for shorter pulse widths. Figure 2 also shows that the CE saturation is more prominent for shorter pulse widths. This can be correlated to appearance of dip at the center of the UTA at shorter laser pulse widths. The reduction in CE and lack of self-absorption dip for longer pulse widths could due related to significant energy loss to plasma hydrodynamic motion,[15] which reduces the temperature of the plasma. White *et al.* reported the role of pulse width (7–40 ns) on CE using a simplified one-dimensional calculation using 1064 nm excitation and 0.9×10^{11} W/cm^2 and showed that the maximum CE was obtained at a pulse duration of 10 ns. It was argued that the in-band energy increases with increased pulse duration, but the CE ultimately decreases beyond 10 ns because of the greater laser energy required to heat the plasma to the optimum electron temperature. Our results showed that the optimum CE is observed for shortest pulse width used and the optimum laser intensity requirement is different for various pulse widths.

We also monitored the EUV emission at 90° with respect to the target normal for investigating the angular effects of EUV emission. The self-absorption properties of the plasma changes with plasma temperature and hence more re-absorption can be expected at the wings because of the presence of colder plasma. Fig. 5 displays the CE for various laser pulse width when measured from side direction with respect to the target normal. One can see that, at 90° the observed CE is significantly lower compared to the recorded values at 45° (Fig. 2) for all pulse widths. Similar to 45° observations, the maximum CE is measured for 5 ns pulse width. However, in this case, the peak in the CE curve has shifted towards lower laser energy. Since plasma is optically thick[8] along the side direction the CE reduces and follows a different trend with laser pulse width and energy[15] as compared to the front direction. The observed saturation or reduction in CE in plasmas at higher energies could be due to opacity effects.[8] It should be noted that we are estimating CE by integrating over 2π sr and assuming the EUV radiation is isotropic. However, Morris *et al.*[25] reported that the in-band emission intensity was relatively constant up to an angle of 60° from the target normal, beyond which it dropped steeply.

Fig. 6 displays the EUV spectra for two different laser pulse widths recorded at 90° with respect to target normal for 5 and 10 ns pulse widths at a fixed intensity. The EUV spectra recorded from the side shown in Fig. 6 will depend on the spatial hydrodynamic and plasma evolutions which in turn strongly depend on laser beam spot, energy, and duration. The spectral intensity is significantly lower at 90° observation compared to 45° observation indicating strong angular dependence. Also the dip structure around the 13.5 nm is not seen in any of these spectra. This indicates that the EUV radiation is heavily absorbed by the optically thick[8] cold plasma in this wings.

B. FC ion analysis

Previous studies showed[26] that the core Sn ions that contributing the UTA at 13.5 nm range from Sn^{10+} to Sn^{13+},

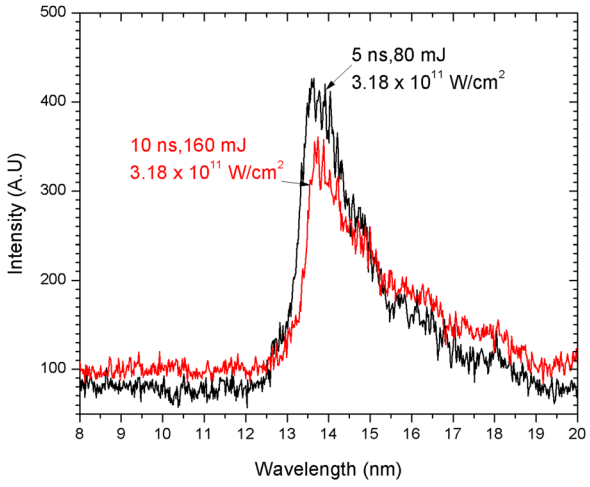

FIG. 6. EUV spectra for two different laser pulse widths recorded from the side of the plasma plume.

while lower-charged species Sn^{6+}–Sn^{9+} emit at the longer-wavelength side of the UTA (>14 nm). So the changes in spectral properties with varying pulse width and laser intensity can also be related to changes in Sn ion populations in the plasma. It is also well known that LPP light sources release debris in the forms of energetic ions, neutral particles, molten droplets, and out-of-band emission.[27] Energetic ionized and neutral particle flux cause sputtering and implantation into the ML mirror coating, lowering its reflectivity.[28] Several mitigation schemes have been proposed to improve the lifetime of the ML mirror, for example, using magnetic fields,[29] a gas curtain,[20,30] low energy prepulses,[31] and mass-limited targets.[32,33] We used FC for evaluating the role of pulse width and laser intensity on the ion emission from LPP. FCs are one of the simplest methods for analyzing ions from LPPs. However, they provide an integrated ion signal containing all charge states, and space charge effects could distort the FC signal.[34] Nevertheless, it is a very useful tool for obtaining the integrated ion flux, the velocity of the ions, and hence, the KE distribution.

Typically, the ion time-of-flight (TOF) profile is represented by a sharp prompt peak, followed by a broad slower peak.[19] The fast prompt peak in the ion signal is caused by the photoelectric effect and can be used as a time marker.[19] Fig. 7 shows the ion kinetic energy profiles obtained from the TOF profiles at various laser energies for four different laser pulse widths used. For this measurement, the FC was positioned at 15 cm from the plasma at an angle of 10° with respect to the target normal. It should be mentioned that space charge effects could distort the FC signal, leading to errors in the estimation of the peak KEs.[34] It was shown that the electrons play an important role in the space charge distortion phenomena.[34] It can be seen from the figure that the ion energy spread reduces with the increase in laser pulse width. One can also see from Fig. 7 that the ion most probable KE reduces with the increase in laser pulse width. The shift in ion KE profile to higher energy side for shorter pulse width could be due to efficient plasma reheating.

The estimated maximum probable velocities from ion TOF profiles are given in Fig. 8 for various pulse widths and laser energies. One can see from Fig. 8 that for the same laser energy, as the pulse width increases the ion velocity reduces. Therefore, with the shorter laser pulse width, we are generating higher energy ions. In LPPs, the ions with higher charge state will have higher KE because of the space charge effect. We also obtained highest CE for shortest pulse width used (5 ns) and it can be related to the increased maximum probable velocities (higher KE) recorded in the case of 5 ns pulse width. As mentioned earlier for generating optimal CE emission conditions, the plasma should be populated by Sn ions with charge state 10^{+}–13^{+}. The average charge state Z of an LPP is related to ion kinetic energy (E) and plasma temperature (T_e) through the relation[35] $E = 5(Z+1)\ T_{e.}$, where E and T_e are in eV. An estimate of average ionization state was made at a laser energy of 120 mJ, assuming $T_e = 30$ eV for all pulse widths used and found that the average charge state dropped from 13 to 7 when the laser pulse width increased from 5 ns to 20 ns. Hence, shorter pulses provide efficient laser-plasma heating leading to the generation of higher charged Sn species indicated by shifted KE profiles to higher energy side which emit efficiently in the in-band region. Fig. 9 displays the measured ion flux for four different laser pulse widths used as a function of laser energy. Regardless of the laser pulse width used for excitation, the ion fluence increased with increasing laser energy. O'Connor *et al.*[23] noticed similar effects at a fixed laser width and their studies showed both the number and the energy of ions increased with applied laser energy.

One can see from Fig. 9 that ion flux remains almost constant for various laser pulse width except at higher

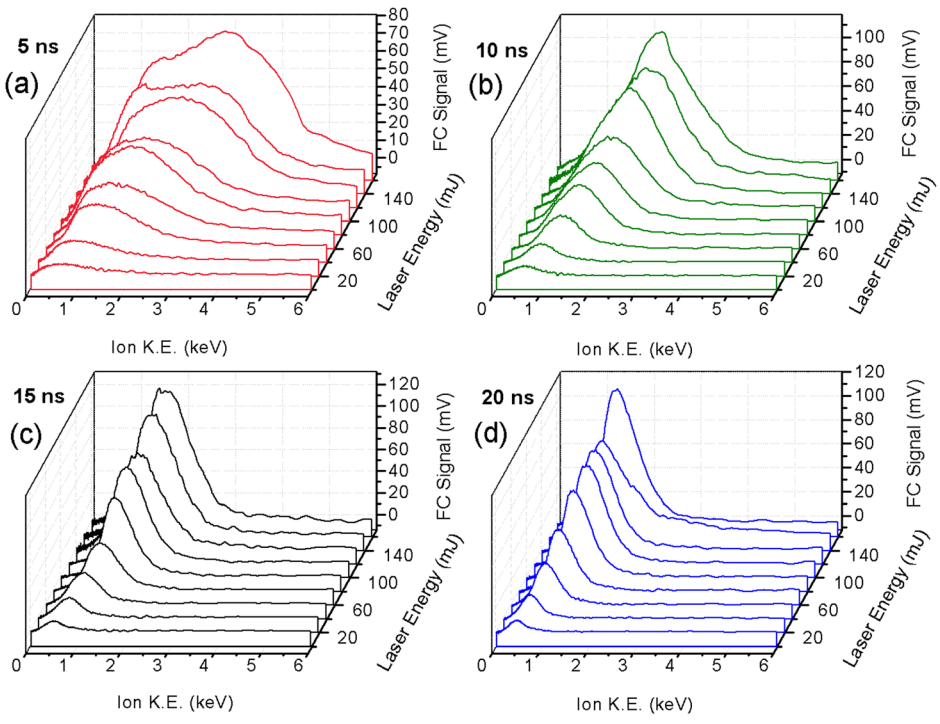

FIG. 7. The estimated kinetic distribution obtained from the TOF ion signal with various laser energies for (a) 5 ns laser pulse width, (b) 10 ns laser pulse width, (c) 15 ns laser pulse width, and (d) 20 ns laser pulse width. For these measurements, the FC is positioned at 15 cm from the target at an angle 10°.

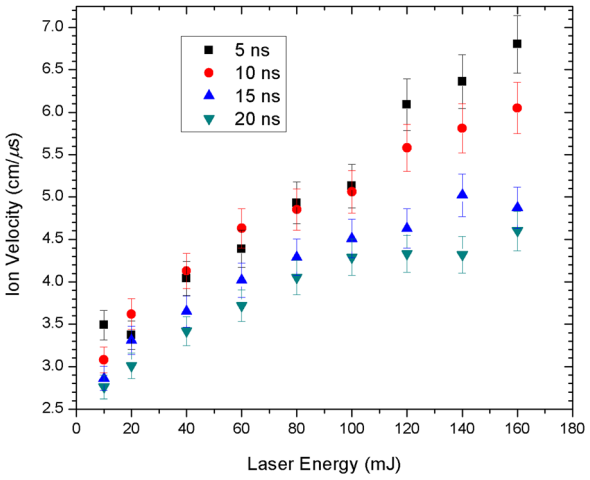

FIG. 8. The estimated most probable ion velocity for various laser pulse widths as a function of laser energy.

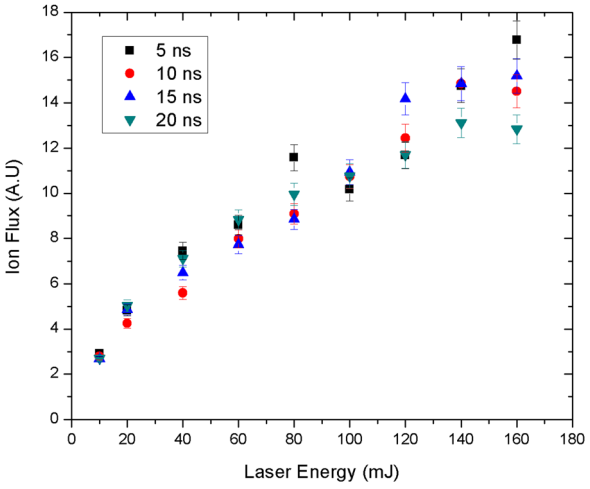

FIG. 9. The estimated ion flux for four different laser pulse widths as a function of laser energy. For these measurements, the FC is positioned at 15 cm from the target at an angle 10°.

energies. It has to be mentioned here that to maximize EUV production we need a plasma with appropriate ion populations, which depended strongly on plasma density and temperature conditions, that emit EUV for longest possible period of time.[36] Typically, tin laser plasmas heated to 30 eV temperatures efficiently emit EUV radiation at 13.5 nm. Lower temperature plasmas contain ion distributions of lower average charge state than those from higher temperature plasmas giving to broader UTA[37] and ions with lower KEs.

IV. SUMMARY

Dependence of EUV spectral emission and ion debris features, of Nd:YAG laser generated Sn plasma on laser pulse duration was experimentally investigated. The CE of the EUV radiation has been shown to depend strongly on laser energy as well as pulse width. The maximum CE of ~2.0% was attained for shortest pulse width used (5 ns) in the parameters range we studied. It was found that the peak CE reduces with the increase in the laser pulse duration. The CE has a tendency to saturate at higher laser intensity; however, the point of saturation differs for various laser pulse widths. The dip structure in EUV spectra caused by absorption of 13.5 nm light by a plasma surrounding an EUV emission region is very prominent for 5 ns laser pulse width as compared to the higher laser pulse width. The EUV emission features also showed strong angular dependence when measured at 90° to target normal. These results indicate the plasma is re-absorbing significant portion of the emitted EUV radiation in the wings.

FC analysis of Sn plasma ion emission was used to generate ion and KE profiles. The maximum probable KEs and ion flux depend on the laser energy and pulse width. It was found that the ion flux increases with laser energy, however, remains more or less constant regardless of pulse width. It was found that the larger duration laser pulse exhibits a much narrower kinetic profile for a fixed laser energy. The most probable ion velocity reduces with increased laser pulse duration. The experimental results suggest that for shorter duration laser pulse higher energy ions are generated due to efficient laser-plasma heating leading to better CE.

ACKNOWLEDGMENTS

This work was supported in part by the U.S. National Science Foundation (PIRE project) and the Academy of Sciences of the Czech Republic and the Czech Republic's Ministry of Education, Youth and Sports, under Projects HiLASE (CZ.1.05/2.1.00/01.0027), DPSSLasers (CZ.1.07/2.3.00/20.0143), and Postdok (CZ.1.07/2.3.00/30.0057), co-financed from the European Regional Development Fund.

[1]J. White, G. O'Sullivan, S. Zakharov, P. Choi, V. Zakharov, H. Nishimura, S. Fujioka, and K. Nishihara, Appl. Phys. Lett. **92**, 151501 (2008).
[2]J. White, P. Dunne, P. Hayden, and G. O'Sullivan, J. Appl. Phys. **106**, 113303 (2009).
[3]S. Yuspeh, K. L. Sequoia, Y. Tao, M. S. Tillack, R. A. Burdt, and F. Najmabadi, Appl. Phys. Lett. **96**, 261501 (2010).
[4]Y. Ueno, G. Soumagne, A. Sumitani, A. Endo, and T. Higashiguchi, Appl. Phys. Lett. **91**, 231501 (2007).
[5]S. Yuspeh, Y. Tao, R. A. Burdt, M. S. Tillack, Y. Ueno, and F. Najmabadi, Appl. Phys. Lett. **98**, 201501 (2011).
[6]R. Rakowski, J. Mikołajczyk, A. Bartnik, H. Fiedorowicz, F. de Gaufridy de Dortan, R. Jarocki, J. Kostecki, M. Szczurek, and P. Wachulak, Appl. Phys. B: Lasers Opt. **102**, 559–567 (2011).
[7]A. Sasaki, A. Sunahara, H. Furukawa, K. Nishihara, S. Fujioka, T. Nishikawa, F. Koike, H. Ohashi, and H. Tanuma, J. Appl. Phys. **107**, 113303 (2010).
[8]S. Fujioka, H. Nishimura, K. Nishihara, A. Sasaki, A. Sunahara, T. Okuno, N. Ueda, T. Ando, Y. Tao, Y. Shimada, K. Hashimoto, M. Yamaura, K. Shigemori, M. Nakai, K. Nagai, T. Norimatsu, T. Nishikawa, N. Miyanaga, Y. Izawa, and K. Mima, Phys. Rev. Lett. **95**, 235004 (2005).
[9]V. Bakshi, *EUV Lithography* (SPIE and John Wiley & Sons, Inc., Bellingham, WA/Hoboken, NJ, 2009).
[10]A. Z. Giovannini and R. S. Abhari, J. Appl. Phys. **114**, 033303 (2013).
[11]I. C. E. Turcu and J. B. Dance, *X-Rays from Laser Plasmas: Generation and Applications* (Wiley, West Sussex, England, 1999).
[12]S. S. Harilal, J. Appl. Phys. **102**, 123306 (2007).
[13]E. Parra, I. Alexeev, J. Fan, K. Y. Kim, S. J. McNaught, and H. M. Milchberg, Phys. Rev. E **62**, R5931 (2000).
[14]M. Schnürer, S. Ter-Avetisyan, H. Stiel, U. Vogt, W. Radloff, M. Kalashnikov, W. Sandner, and P. V. Nickles, Eur. Phys. J. D **14**, 331–335 (2001).

[15]T. Ando, S. Fujioka, H. Nishimura, N. Ueda, Y. Yasuda, K. Nagai, T. Norimatsu, M. Murakami, K. Nishihara, N. Miyanaga, Y. Izawa, and K. Mima, Appl. Phys. Lett. **89**, 151501 (2006).
[16]K. L. Sequoia, "Extreme-ultraviolet radiation transport in small scale length laser-produced tin plasmas," Ph.D. dissertation (University of California, San Diego, 2009).
[17]Y. Tao, Y. Ueno, S. Yuspeh, R. Burdt, M. S. Tillack, and F. Najmabadi, Proc. SPIE **7969**, 796930 (2011).
[18]Y. Ueno, T. Ariga, G. Soumagne, T. Higashiguchi, S. Kubodera, I. Pogorelsky, I. Pavlishin, D. Stolyarov, M. Babzien, K. Kusche, and V. Yakimenko, Appl. Phys. Lett. **90**, 191503 (2007).
[19]R. W. Coons, S. S. Harilal, D. Campos, and A. Hassanein, J. Appl. Phys. **108**, 063306 (2010).
[20]T. Wu, X. Wang, H. Lu, and P. Lu, J. Phys. D: Appl. Phys. **45**, 475203 (2012).
[21]O. Morris, A. O'Connor, E. Sokell, and P. Dunne, Plasma Sources Sci. Technol. **19**, 025007 (2010).
[22]R. A. Burdt, Y. Tao, M. S. Tillack, S. Yuspeh, N. M. Shaikh, E. Flaxer, and F. Najmabadi, J. Appl. Phys. **107**, 043303 (2010).
[23]A. O'Connor, O. Morris, and E. Sokell, J. Appl. Phys. **109**, 073301 (2011).
[24]T. Higashiguchi, M. Kaku, M. Katto, and S. Kubodera, Appl. Phys. Lett. **91**, 151503 (2007).
[25]O. Morris, P. Hayden, F. O'Reilly, N. Murphy, P. Dunne, and V. Bakshi, Appl. Phys. Lett. **91**, 081506 (2007).
[26]A. Cummings, G. O'Sullivan, P. Dunne, E. Sokell, N. Murphy, and J. White, J. Phys. D: Appl. Phys. **38**, 604 (2005).
[27]S. S. Harilal, B. O'Shay, Y. Tao, and M. S. Tillack, Appl. Phys. B: Lasers Opt. **86**, 547 (2007).
[28]J. P. Allain, M. Neito, M. R. Hendricks, P. Plotkin, S. S. Harilal, and A. Hassanein, Rev. Sci. Instrum. **78**, 113105 (2007).
[29]Y. Ueno, G. Soumagne, A. Sumitani, A. Endo, T. Higashiguchi, and N. Yugami, Appl. Phys. Lett. **92**, 211503 (2008).
[30]S. Bollanti, F. Bonfigli, E. Burattini, P. Di Lazzaro, F. Flora, A. Grilli, T. Letardi, N. Lisi, A. Marinai, L. Mezi, D. Murra, and C. Zheng, Appl. Phys. B: Lasers Opt. **76**, 277 (2003).
[31]Y. Tao, M. S. Tillack, S. S. Harilal, K. L. Sequoia, and F. Najmabadi, J. Appl. Phys. **101**, 023305 (2007).
[32]S. S. Harilal, B. O'Shay, M. S. Tillack, and Y. Tao, J. Phys. D: Appl. Phys. **39**, 484 (2006).
[33]T. Okuno, S. Fujioka, H. Nishimura, Y. Tao, K. Nagai, Q. Gu, N. Ueda, T. Ando, K. Nishihara, T. Norimatsu, N. Miyanaga, Y. Izawa, K. Mima, A. Sunahara, H. Furukawa, and A. Sasaki, Appl. Phys. Lett. **88**, 161501 (2006).
[34]R. Janmohamed, G. Redman, and Y. Y. Tsui, IEEE Trans. Plasma Sci. **34**, 455 (2006).
[35]Y. B. Zeldovich and Y. P. Raizer, *Physics of Shock Waves and High-Temperature Hydrodynamic Phenomena* (Dover, New York, 2001).
[36]A. Hassanein, V. Sizyuk, T. Sizyuk, and S. S. Harilal, J. Micro/Nanolithogr., MEMS, MOEMS **8**(4), 041503 (2009).
[37]J. R. Freeman, S. S. Harilal, B. Verhoff, A. Hassanein, and B. Rice, Plasma Sources Sci. Technol. **21**, 055003 (2012).